Holographic techniques at long wave infrared wavelengths

Jean-François Vandenrijt, Marc Georges, mgeorges@ulg.ac.be
Centre Spatial de Liège, Université de Liège, Avenue du Pré-Aily, B-4031 Angleur, Belgium.

ABSTRACT

For industrial applications, holographic interferometry and electronic speckle pattern interferometry techniques using visible laser light are often too sensitive to external perturbations. Consequently they require too much stability, preventing their widespread use in field applications. One simple idea to overcome this problem is to increase the wavelength of the laser light. We considered the 10 µm wavelength range corresponding to well known CO_2 laser and because imagers exist in this spectral range. One other important advantage is that the strain/displacement measurement range is larger than the equivalent techniques in visible light.We will present the preliminary experiences performed so far with components available in our lab. Mainly, we show in-plane electronic speckle pattern interferometry and for the first time digital holographic interferometry. We also discuss specific problems related to the wavelength increase.

INTRODUCTION

Holographic interferometry (HI) and electronic speckle pattern interferometry (ESPI) metrology techniques [1] in visible light are not often well suited for field applications due to the short wavelength used, which imposes high stability constraints. For that reason, owing to a self-referenced principle of working, shearography imposes itself for industrial and field applications but mainly for detection of defects. For displacement metrology, both the other techniques are preferable. One way to decrease their sensitivity to external perturbations is to use a longer wavelength. Our purpose is to investigate the applications of those techniques in LWIR, and more specifically at 10 µm which correspond to the well known CO_2 laser. This shall provide us a typical 20 factor of decrease of the stability requirements, meantime the range of measurement shall be also increased by the same factor.

The most important element for performing holography is to use an adequate recording medium. Infrared holography in the 10 µm range is not a new subject. Back in the seventies, several groups investigated different materials for that effect. The first evidence of research in this field were made by Simpson and Deeds who considered liquid crystals for recording at 10.6 µm and readout with HeNe laser [2]. The works that followed used the same separated wavelengths for recording and readout but applied to recording media: wax and gelatin films [3], thermochromic materials [4]. At that period, Canadian researchers made a lot of work in this field and they considered several materials and presented applications. They considered acrylic and thin films [5], wax [6,7], oil films deposited on glass plates [8]. Investigations were stopped and restarted later with new materials like resist [9], tetrafluoroethylene [10] and PAA films [11]. More recently, Calixto showed the use of organic materials for recording images and gratings at 10.6 µm [12].

All these materials are able to record patterns through relief variation, producing phase holograms that are processable in situ. Also they show relatively good figures of merit in term of diffraction efficiency. But what seems to remain limited is the resolution of such media with rapid drop of diffraction efficiency for line spacing larger than 10 lines/mm. Also they all use visible wavelengths for readout which does not make easy the application of these materials for real-time holographic interferometry. Instead double-exposed holograms, if they are readout with visible lasers, can be envisaged but this procedure is more restrictive in applicability. A few of these papers dealt with application in HI, mainly considering shift of phase elements, which is a very limited application of HI, moreover with poor quality of interferograms [8,11].

After this review of past work, our conclusion was that no convincing photosensitive material exists for HI at

10 µm and we decide to investigate the possibility of electronic hologram recording. We here refer to techniques that are known as electronic speckle pattern interferometry (ESPI), TV-Holography and the more recent digital holographic interferometry. The very first evidence of using electronic hologram recording at 10 µm was made in 2003 by Allaria et al. [13] who proposed digital holography and show reconstruction of Fresnel digital holograms of a 700 µm mask object placed in a Mach-Zehnder interferometer configuration. Although pioneering in the field, this work is not really oriented to show displacements like with ESPI and digital HI.

In this paper we show, the application of electronic hologram recording for measuring in-plane, and for the first time to the best of our knowledge out-of-plane displacements as well as the application of digital holographic interferometry of opaque objects at 10 µm.

IN-PLANE ESPI SET-UP AND RESULTS

At the beginning of our investigations, we were limited to a commercial thermal camera that is normally used for thermography by other colleagues. Therefore we were not allowed to dismantle it for a flexible set-up. Thus we had to reject the idea of an optical configuration for out-of-plane ESPI measurement.

In a previous paper [14], we have presented our early experiments using in-plane ESPI. We discussed one of the main problem which is related to the scattering properties of the object when illuminated with 10 µm wavelength laser. Indeed at higher wavelengths the objects reflectivity is much more specular than at lower wavelengths. Therefore a specular peak is more easily visible and intense in LWIR than in visible. We showed that in the in-plane set-up, presented in Figure 1 and Figure 2, we avoid the observation of the specular peak due to the hight incidence angle of the illumination. For enhancing the scattering reflectivity, we applied to the object a white removable powder like the one used with visible light. Besides the intense specular peak, a sufficient level of scattered speckled light can be used for recording interference pattern at the camera level. The object is a metallic plate whose movement is a rotation around its normal (z-axis). It was illuminated by two beams at symmetric incidence angles (45°).

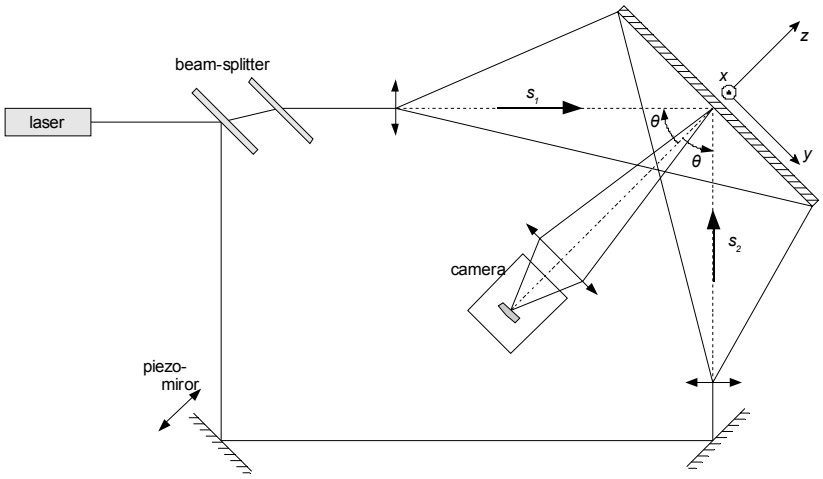

Figure 1: Experimental set-up schema for in-plane ESPI observation.

The beam-splitter is composed of two wedge plates. The first split the incident beam into a reflected and a refracted beam. The second one compensates the light beam deviation of the refracted beam introduced by the first one. One of the mirrors is mounted on a piezo-electric translator for application of the phase-shifting technique.

The camera used is a FLIR ThermaCAM™ S45 using an uncooled microbolometer array of 320×240 pixels. Its maximum thermal sensitivity is in the 7.5 to 13 µm spectral range. The objective lens has a focal length of 35 mm and the minimum distance of object is 30 cm. The f-number is not adjustable so the speckle size is fixed. However, due to the longer wavelength, the latter was clearly visible on the image. For the illumination, we used a CO_2 laser emitting at 10 µm.

This set-up allowed us to realize in-plane displacement measurements successfully. It was the first time to our knowledge that such observation on opaque object was performed, providing so the first proof of the feasibility of such technique at 10 µm. An example of observation made was that of the rotation of the aluminum plate and is shown in Figure 3 and Figure 4. The plate was covered with reflecting powder to produce speckle. The first four images shows the interferograms obtained by phase-shifting, realized with the piezo-mounted mirror. The computed phase angle and unwrapped phase can be used to measure the displacements of the plate, thus the rotation angle applied. A more complete description of the results is presented in reference [14].

(a) (b) (c)

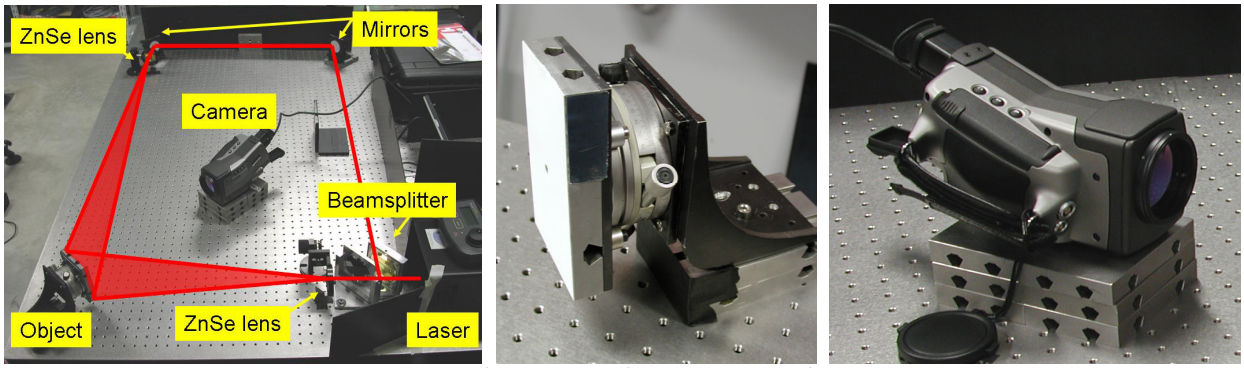

Figure 2: (a) Experimental set-up for in-plane ESPI observation of an aluminum plate (b) with a commercial thermographic camera (c).

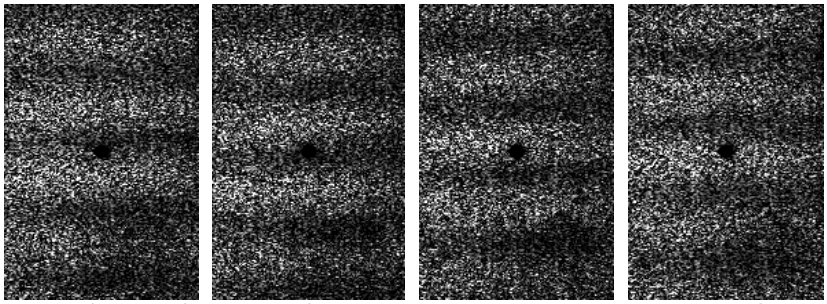

Figure 3: The four interferograms of the aluminum plate observed in in-plane ESPI with a ¼ wavelength phase-shift between each acquisition.

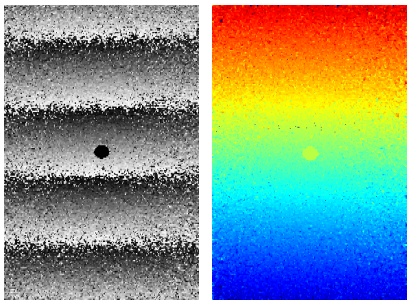

Figure 4: Reconstructed phase value wrapped and unwrapped, using phase-stepping ESPI in-plane.

OUT-OF-PLANE ESPI SET-UP AND RESULTS

After the first experiment of in-plane ESPI, we were allowed to use an infrared camera without imaging objective, giving easy access to the sensor plane throught small modifications. This opened the door to out-of-plane ESPI and digital holography which require the use of a beam combiner placed in front of the imaging sensor. We first started the out-of-plane ESPI technique. The set-up we used is shown in Figure 5 and Figure 6.

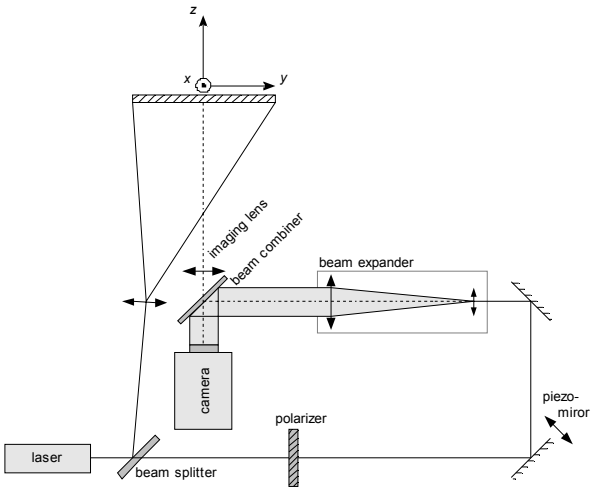

Figure 5: Scheme of the experimental set-up for out-of-plane LWIR ESPI.

In order to equalize the light fluxes on the detector, the beam-splitter we used is a semi-reflective plate, reflecting 90% of the light intensity and transmitting 10%. A polarizer is used to adjust the intensity of the reference beam on the sensor. Like in in-plane ESPI, one of the mirror has been mounted on a piezo-electric translator for application of the phase-shifting. A beam-expander is used to produce a plane reference beam on the detector. The camera we used is a Jade II LWIR from CEDIP Infrared Systems, with a 320 × 240 pixels sensor. Its sensitivity is mainly situated in the 8–9.5 µm wavelength range. As the laser is emitting at 10.6 µm, we are not in the main sensitivity range. However, the sensitivity appeared to be sufficient for our observations. To be able to insert a beam combiner between the sensor and the imaging lens in front of it, we have disassembled the camera front cover and mounted the sensors on a metallic plate (see right picture in Figure 6).

The comment that we gave about specular reflection in the in-plane set-up is also a bigger problem for the out-of-plane set-up. Indeed the object is illuminated with a beam which is ideally coaligned with optical axis of the camera. Here the object has been slightly rotated to avoid the specular peak entering the sensor. It is then not present in the images.

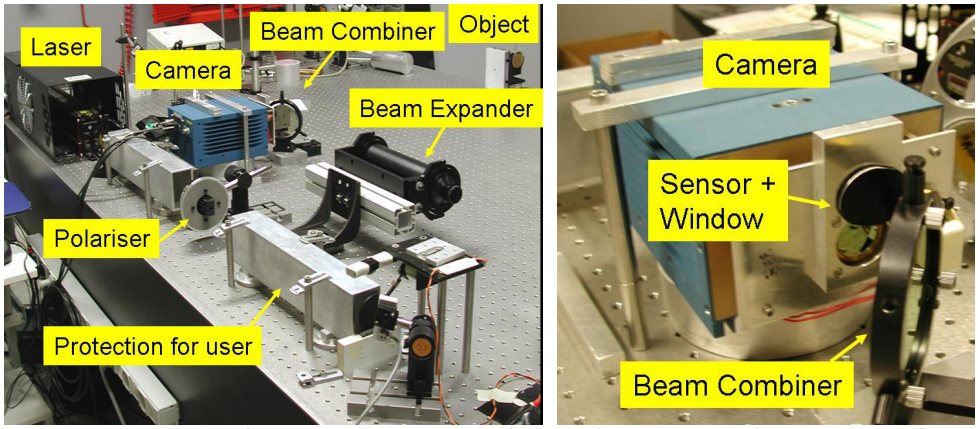

Figure 6: (a) Picture of the experimental set-up for out-of-plane LWIR ESPI with detail of the camera assembly (b).

Because the camera sensor is of an old generation and partially damaged on part of its surface, the performances were reduced. Although the sensor has a higher number of pixels, the images produced were of lower quality than with the other thermographic camera. However, it has been sufficient to carry out displacements measurements successfully. This can be seen in the observation of the rotation displacement shown in Figure 7 and Figure 8.

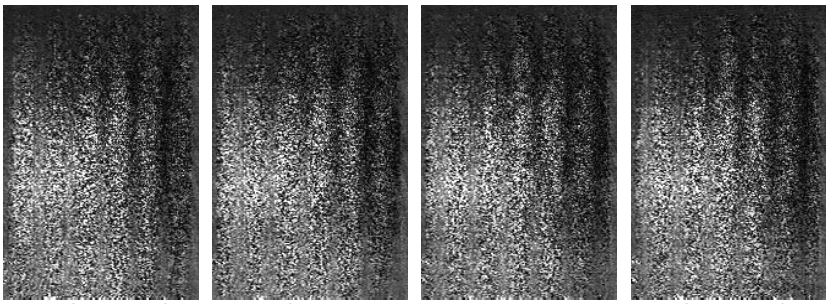

Figure 7: The four interferograms of the aluminum plate observed in out-of-plane ESPI with a ¼ wavelength phase-shift between each acquisition.

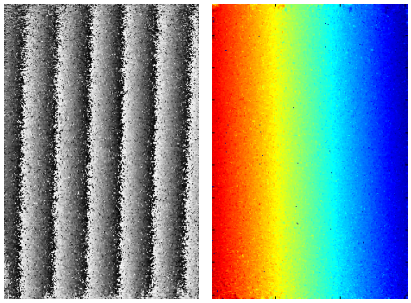

Figure 8: Reconstructed phase value wrapped and unwrapped, using phase-stepping ESPI out-of-plane.

DIGITAL HOLOGRAPHY SET-UP AND RESULTS

Performing digital holography at 10 µm is not a premiere. Such an experiment has already been accomplished by Allaria et al. [13]. However, their work consist in digital reconstruction of a hologram of a transparency mask with 700 nm holes, in a Mach-Zender configuration. To the best of our knowledge, no demonstration of digital holography in LWIR has been performed on opaque scattering objects for the purpose of displacement measurement.

The experimental set-up used is the same as the set-up used for out-of-plane ESPI where, the imaging lens in front of the camera has been removed and the phase-shifting piezo-translator unused (see Figure 9). The reconstruction of the image is realized by software in quasi-real time. A shutter has also been added, in order to obtain the object wavefront to enhance the reconstructed images using the HRO subtraction [15]. For further enhancement, we have also suppressed the DC-term in the reconstructed images [16].

The maximum admissible angle between object wave and reference wave $\gamma_{\max}$ is given by [1]:

$$\gamma_{\max} = 2 \arcsin\left(\frac{\lambda}{4\,\Delta}\right)$$

where λ is the wavelength and Δ the pitch of the detector, which is equal to 30 µm for our camera. Compared to digital holographic set-up in visible, the larger pixel size here is partially compensated by the wavelength increase. This gives a maximum admissible angle of the order of ~ 10 degrees. Examples of images realized using digital holography at 10 µm can be seen in Figure 10 and Figure 11. In figure 10, one clearly observes the zero-order peak and both first orders corresponding to real and virtual images. Figure 11 shows only the real image reconstructed.

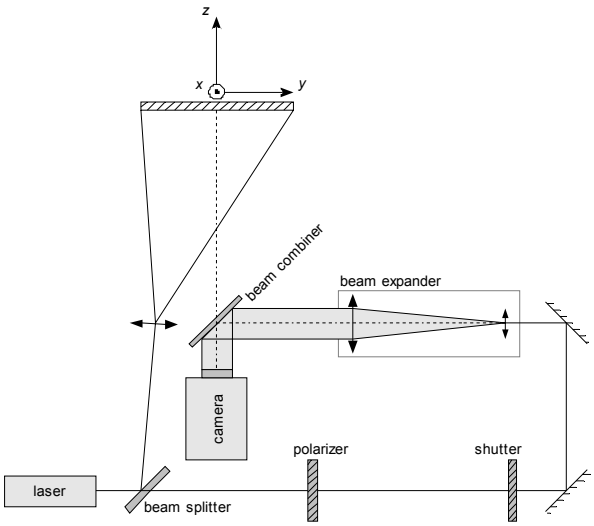

Figure 9: Experimental set-up for LWIR digital holographic interferometry.

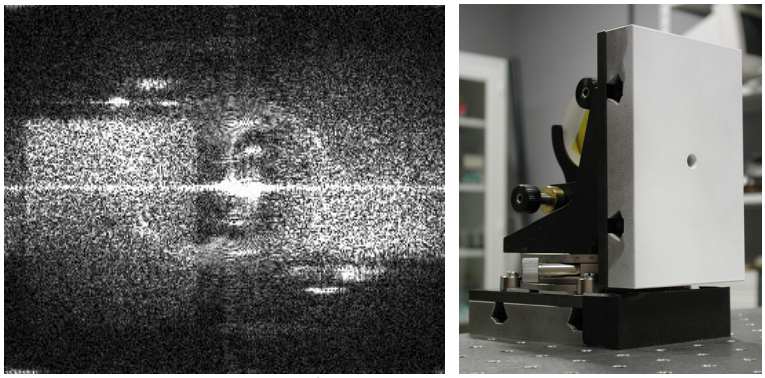

Figure 10: (a) Reconstructed image of the aluminum plate acquired by digital holography compared to the original object, on the right.

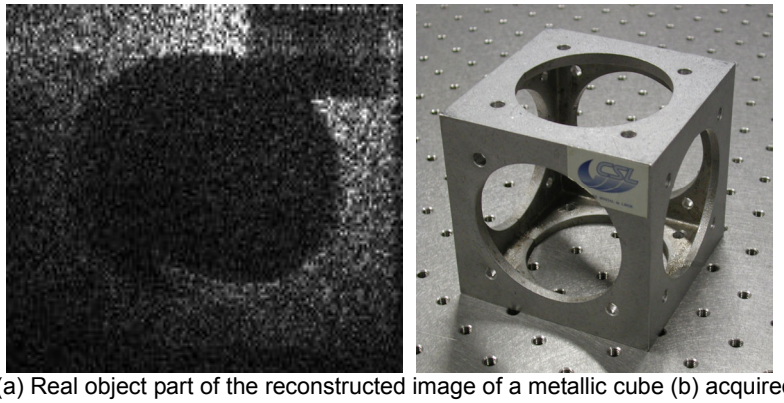

Figure 11: (a) Real object part of the reconstructed image of a metallic cube (b) acquired by digital holography compared to the original object, on the right.

After the successful reconstruction of object intensities, we have investigated the phase information provided in the reconstructed images. For this experiment, we have observed the rotation of the same aluminum plate than in the previous ESPI experiments. The methodology used for the phase angle determination is described in Figure 12.

Because of the restrictions imposed by the digital holography technique, the displacements measurements realized were of lower resolution and noisier. However, we could successfully compute the rotation angle for low

rotation and compare it to values obtained with counter-measurements with a theodolite. An example of such a measurement is shown in Figure 13.

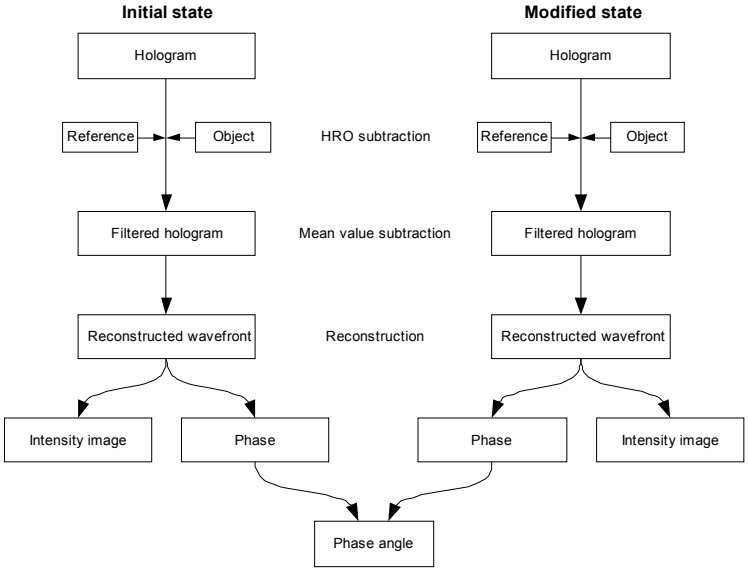

Figure 12: Phase angle determination using digital holography.

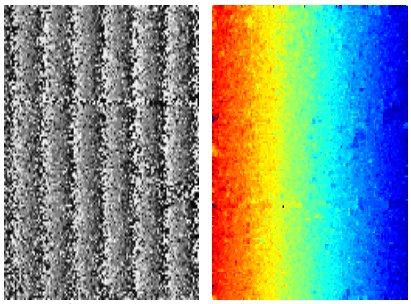

Figure 13: Computed phase interferogram and the unwrapped displacement map obtained by digital holography at 10 µm.

CONCLUSIONS

We have exposed the methodology used to achieve in-plane and out-of-plane ESPI , as well as digital holography observations at 10 µm. We have then shown our first results, demonstrating the feasibility of those techniques in the LWIR spectrum. The higher specular reflectivity property of objects when illuminated with larger wavelength for a given roughness) was not a real problem but required to avoid the specular peak not entering the imaging system of the thermographic camera. However in the future we will have to improve the technique of the technique to render it less immune to this.

The performances we obtained obviously need to be improved for industrial applications, but they are only a first step in the exploration of holographic interferometry techniques at 10 µm, showing promising outcomes. New projects start at the time of writing this paper and which will allow us to study in deep all specificities of holography at LWIR wavelengths and to develop optimized set-up with dedicated optics and state-of-the-art camera and components.

REFERENCES

[1] T. Kreis, Holographic Interferometry – Principles and Methods, Vol. 1, Akademie Verlag Series in optical metrology, Berlin (1996).

[2] W.A. Simpson, W.E. Deeds, “Real-time visual reconstruction of infrared holograms”, Appl. Opt. 9(2), 499-501 (1970).

[3] S. Kobayashi, K. Kurihara, "Infrared Holography with Wax and Gelatin Film", Appl. Phys. Lett. 19, 482-484 (1971).

[4] R.R. Roberts, T.D. Black, “Infrared holograms recorded at 10.6 μm and reconstructed at 0.6328 μm”, Appl. Opt. 15(9), 2018-2019 (1976).

[5] M. Rioux, M. Blanchard, M. Cornier, R. Beaulieu, D. Bélanger, “Plastic recording media for holography at 10.6 μm”, Appl. Opt. 16 (7), 1876-1879 (1977).

[6] R. Beaulieu, R. A. Lessard, M. Cormier, M. Blanchard, and M. Rioux, “Infrared holography on commercial wax at 10.6 μm”, Appl. Phys. Lett. 31, 602-603(1977).

[7] Beaulieu, R. A. Lessard, M. Cormier, M. Blanchard, and M. Rioux, “Pulsed IR holography on takiwax films”, Appl. Opt. 17 (22), 3619-3621 (1978).

[8] J. Lewandowsky, B. Mongeau, and M. Cormier, “Real time interferometry using IR holography on oil films”, Appl. Opt. 23, 242-246 (1984).

[9] R. Beaulieu, R. A. Lessard, and S. Ling Chin, “Resist recording media for holography at 10.6 mm” in Photopolymers and applications in holography, optical data storage, optical sensors, and interconnects, Proc. SPIE 2042, 259-263 (1994).

[10] R. Beaulieu, R. A. Lessard, and S. Ling Chin, “Recording of infrared radiation (10.6 μm) in a tetrafuoroethylene copolymer of vinylidene fluoride”, Proc. of the International Conference on Lasers 94, 758-762 (1994).

[11] R. Beaulieu, R. A. Lessard, “Infrared holography on poly(acrylic acid) films”, in Applications of Photonic Technology 4 (Photonics North 2000), Proc. SPIE 4087, 1298-1301 (2000).

[12] S. Calixto, “Albumen as a Relief Recording Media for Spatial Distributions of Infrared Radiation. Fabrication of Interference Gratings and Microlenses”, Appl. Opt. 42, 259-263 (2003).

[13] E. Allaria, S. Brugioni, S. De Nicola, P. Ferraro, S. Grilli, R. Meucci, “Digital Holography at 10.6 μm”, Opt. Commun. 215, 257-262 (2003).

[14] J.-F. Vandenrijt, M. Georges, "Infrared Electronic speckle pattern interferometry at 10 μm", Proc. SPIE 6616 (2007).

[15] Ø. Skotheim, "HoloVision: a software package for reconstruction and analysis of digitally sampled holograms", Proc. of SPIE 4933, p. 311-316 (2003).

[16] T. Kreis, W. Jüptner, "Suppression of the DC term in digital holography", Opt. Eng. 36, p. 2357-2360 (1997).